AD-A070 946   ENVIRONMENTAL RESEARCH AND TECHNOLOGY INC   CONCORD MASS   F/G 4/2
               METEOROLOGICAL DATA ANALYSES IN SUPPORT OF THE ABRES PROGRAM.(U)
               JAN 79   K R HARDY   F19628-76-C-0069
UNCLASSIFIED   ERT-P-1996-F   AFGL-TR-79-0084   NL

| OF |
AD
A070946

END
DATE
FILMED
8 --79
DDC

1.0

1.1

1.25

4.5
5.0
5.6

2.8

3.2

3.6

4.0

2.5

2.2

2.0

1.8

1.4   1.6
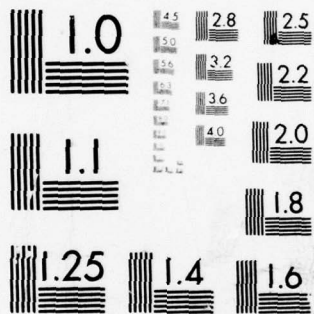
MICROCOPY RESOLUTION TEST CHART
NATIONAL BUREAU OF STANDARDS-1963-A

AFGL-TR-79-0084

METEOROLOGICAL DATA ANALYSES IN
SUPPORT OF THE ABRES PROGRAM

Kenneth R. Hardy

Environmental Research & Technology, Inc.
696 Virginia Road
Concord, Massachusetts 01742

January 1979

Final Report
January 1976 - January 1979

Approved for public release; distribution unlimited

AIR FORCE GEOPHYSICS LABORATORY
AIR FORCE SYSTEMS COMMAND
UNITED STATES AIR FORCE
HANSCOM AFB, MASSACHUSETTS 01731

79 07 09 003

SECURITY CLASSIFICATION OF THIS PAGE *(When Data Entered)*

REPORT DOCUMENTATION PAGE	READ INSTRUCTIONS BEFORE COMPLETING FORM

1. REPORT NUMBER	2. GOVT ACCESSION NO.	3. RECIPIENT'S CATALOG NUMBER
AFGL-TR-79-0084		

4. TITLE *(and Subtitle)*	5. TYPE OF REPORT & PERIOD COVERED
Meteorological Data Analyses in Support of the ABRES Program	Final Report Jan 1976 to Jan 1979
	6. PERFORMING ORG. REPORT NUMBER
	ERT-P-1996-F

7. AUTHOR(s)	8. CONTRACT OR GRANT NUMBER(s)
Kenneth R. Hardy	F19628-76-C-0069

9. PERFORMING ORGANIZATION NAME AND ADDRESS	10. PROGRAM ELEMENT, PROJECT, TASK AREA & WORK UNIT NUMBERS
Environmental Research & Technology, Inc. 696 Virginia Road Concord, Massachusetts 01742	627A00BE P.E. 63311F

11. CONTROLLING OFFICE NAME AND ADDRESS	12. REPORT DATE
Air Force Geophysics Laboratory Hanscom AFB, Massachusetts 01731 Monitor/Peter A. Giorgio/LY	January 1979
	13. NUMBER OF PAGES
	27

14. MONITORING AGENCY NAME & ADDRESS *(if different from Controlling Office)*	15. SECURITY CLASS. *(of this report)*
	Unclassified
	15a. DECLASSIFICATION/DOWNGRADING SCHEDULE

16. DISTRIBUTION STATEMENT *(of this Report)*

approved for public release; distribution unlimited

17. DISTRIBUTION STATEMENT *(of the abstract entered in Block 20, if different from Report)*

D D C
RECEIVED
JUL 10 1979
B

18. SUPPLEMENTARY NOTES

19. KEY WORDS *(Continue on reverse side if necessary and identify by block number)*

environmental severity index	radar reflectivity
weather radar measurements	liquid water content estimates
precipitation particle measurements	cross section analysis

20. ABSTRACT *(Continue on reverse side if necessary and identify by block number)*

The Air Force Geophysics Laboratory (AFGL) has been tasked by the Space and Missiles System Organization (SAMSO) to provide meteorological analysis in support of the Advanced Ballistic Reentry Systems (ABRES) Program. The primary objectives of the work carried out under this contract have been to assist AFGL in (1) the analysis of surface, upper air, and satellite data leading to the computation of liquid water content profiles, (2) the analysis of special observational data obtained from aircraft flight experiments, (3) computer analysis of radar data, (4) development of display techniques for the AFGL Liquid Water

DD FORM 1 JAN 73 1473 EDITION OF 1 NOV 65 IS OBSOLETE

SECURITY CLASSIFICATION OF THIS PAGE *(When Data Entered)*

20. ABSTRACT (cont)

Content Analyzer, (5) the evaluation of the uncertainties in the estimation of hydrometeor mass concentrations using radar and aircraft measurements, and (6) the assessment of thin cirrus cloud over the tropical Pacific.

The major results accomplished include (1) the development of improved computer programs for the real-time estimation of liquid water content profiles using radar measurements, (2) the completion of meteorological cross section analyses for Hong Kong, (3) the development of improved techniques for the collection, processing, and display of satellite meteorological data, (4) the establishment of the important error contributions to the uncertainties in the liquid water content estimates; the major contributors to the errors were found to be the radar calibration, polarization effects by the particles, length-to-mass conversion from the particle measurements, distribution estimates, and extrapolation limitations, (5) the establishment of procedures to derive liquid water content profiles from surface, upper air, and satellite data, (6) the development of improved techniques for the derivation of the environmental severity index using visible and infrared brightness values from satellites, and (7) the definition of the concentrations of ice particles which can be detected visually from the surface or from aircraft and by means of an infrared sensor from space.

ACKNOWLEDGMENTS

Accession For	
NTIS GRA&I	✔
DDC TAB	☐
Unannounced	☐
Justification_____	
By_____	
Distribution/	
Availability Codes	
Dist.	Avail and/or special
A	

TABLE OF CONTENTS

LIST OF TABLES AND ILLUSTRATIONS

1. INTRODUCTION

The Air Force Geophysics Laboratory (AFGL) has been tasked by the Space and Missiles System Organization (SAMSO) to provide meteorological analysis in support of the Advanced Ballistic Reentry Systems (ABRES) Program. The primary objectives of the work carried out under this contract by Environmental Research & Technology, Inc. (ERT) have been to assist AFGL in (1) the analysis of surface, upper air, and satellite data leading to the computation of liquid water content profiles, (2) the analyses of special observational data obtained from aircraft flight experiments, (3) computer analysis of radar data, (4) development of display techniques for the AFGL Liquid Water Content Analyzer, (5) the evaluation of the uncertainties in the estimation of hydrometeor mass concentrations using radar and aircraft measurements, and (6) the assessment of thin cirrus cloud over the tropical Pacific.

Throughout the three-year period of the contract, there were six major tasks which were identified as contributing to the support of the ABRES program. These tasks varied widely in their complexity and in their level of effort. This report is intended to provide a summary of each of these tasks.

As a result of the research and analyses on the program, three scientific reports have been published (Crane, 1978; Burke et al, 1978; and Bussey, 1979). These reports provide the details of the most significant scientific contributions accomplished under the contract.

2. ANALYSIS AND SUPPORT

2.1 Task 1 - Support for the AFGL Liquid Water Content Analyzer

Through a contract with Raytheon Company, AFGL developed an instrument to derive real-time estimates of the liquid water content using weather radar data. Support for the maintenance, operation, and for the development of new or improved computer programs for the water content analyzer was provided by ERT for two winter seasons at Wallops Island, Virginia. The analyzer was a key instrument in the assessment of the hydrometeor environment for the Sandia Air Force Materials Study (SAMS) Program.

Documentation of the work completed under this task was given in two working reports. One report was entitled WETHRAD (Weather Radar System) and documented some of the operating system of the analyzer as well as the new programs developed during the 1976 winter season at Wallops Island. The second working report detailed all the changes made in the system during the 1977 winter season and provided an accurate description of all aspects of operating and using the analyzer. Work on the task was terminated at the end of FY 77 when there was no further requirement for use of the analyzer at Wallops Island.

2.2 Task 2 - Support for the McIDAS

This task involved support for the maintenance and modifications to the Man Computer Interactive Data Access System (McIDAS) at AFGL. The primary work accomplished was (1) the completion of the antenna installation including the tests for all drive systems and for printing accuracy, (2) the installation and testing of a sensitive receiver, (3) development of an improved antenna tracking circuit, and (4) modifications to the automated handling of satellite meteorological data in order to acquire information from the mid-west United States. Support on this program was provided for a six-month period and was terminated in July 1976.

2.3 Task 3 - Cloud Data Analysis

The major portion of the work in this task was the analysis of air-
craft measurements of cloud and precipitation particles and the incor-
poration of these measurements with corresponding observations of the
radar structure of the storm as observed with the radar systems at
Wallops Island. Extensive studies were completed on relating the ice
crystal area to ice crystal mass which was then used to determine the
particle distributions and the cloud liquid water content of the ice and
snow crystals. The final matching of the water contents with those
derived from the radar measurements was accomplished through a series of
analysis techniques which had been developed throughout the first year
of the study.

During the third year of the program, the work concentrated on the
mass versus size and mass versus area relationship from Knollenberg's
ice crystal data to find the logarithmic regression equations and the
standard errors to fit Knollenberg's linear functions. Work proceeded
on the derivation of weighting functions of the average projection ratio
channels and the equivalent circle ratio channels for eleven different
ideal crystals.

Particle size data from several aircraft altitudes were processed
and used to compute precipitation growth, and a computer program was set
up to create the appropriate input for computations of ice crystal growth.
Cloud data from twenty-one experimental tests carried out at Wallops
Island and Kwajalein were processed.

A significant part of the effort on this task involved the develop-
ment of computer programs to estimate the probable liquid water contents
of clouds and precipitation using radiosonde data along with visible and
infrared (IR) data from satellites. The liquid water content was then
multiplied by the height and integration of this product was computed to
obtain a parameter called the Environmental Severity Index (ESI). Using a
data base of eleven radiosonde stations, the mean, median, and accumu-
lated frequency tables of ESI were obtained.

Further development on the ESI studies involved taking an existing
computer program (ANYPT), which extracted the mean atmospheric profiles
of temperature, pressure, humidity and density over any point on the

3

globe, and modifying it to extract the mean temperature profiles over the NMC grid points covering the Eurasia area. This new program, entitled PROFIL outputs the profiles generated by ANYPT Program ESRESI was then developed to computer wintertime ESI values; in this program the mean temperature profiles from program ANYPT were used to assist in the discrimination of ice and snow from clouds. Adidtional programs, called PROBMP and TSTATS, have been used operationally to derive statistics of ESI values over Eurasia for the months of May through September 1973.

During the last six months of the project, work involved the processing and analysis of aircraft and radar data from Kwajalein. Major accomplishments were as follows: (1) an organization of both crystal size relationships and crystal area relationships for various particle types was completed, (2) Knollenberg's 2-D crystal data were evaluated manually and a format was developed which made it possible to compare the results with a computerized version of the 2-D data anslysis, (3) the processing of both the AFGL-2 and the satellite data comparison models for the three months of May, July and October 1973 was completed, and (4) a computer program to generate a non-dimensional particle-size distribution, which was subsequently used to obtain the liquid water content, was developed.

2.4 Task 4 - Cross Section Analysis and Liquid Water
     Content Assessment at Kwajalein

Bussey (1978) has prepared a scientific report which describes the methodology for cross section analysis and liquid water content assessment. Since the details of this task are included in the report, only the abstract is given below.

"Analyzing surface and upper air meteorological observations in the form of a time cross section is a concise form of simulating atmospheric conditions over a particular location. Using these observations and DMSP satellite data, procedures for estimating the liquid water content within regions of cloud and precipitation have been derived. The procedures for deriving the liquid water content profiles have evolved over a

4

five-year period, and it is the purpose of this report to describe the current methodology. The profiles of liquid water content are used as input for a determination of the environmental severity index (ESI). The advantage of the technique described is that estimates or a climatology of ESI can be obtained in any part of the world through an analysis of readily available meteorological observations."

2.5 Task 5 - Evaluation of Uncertainties in the Estimation of Hydrometeor Mass Concentrations Using SPANDAR Data and Aircraft Measurements

A major effort under the project was the detailed assessment of uncertainties or errors in the radar and aircraft estimates of cloud and precipitation liquid water contents along the trajectories of reentry test vehicles. Crane (1978) has described the complete results of the work completed under this task. Since this was a major and important part of the overall project, a more detailed description of the task is provided than the descriptions for the previous tasks.

2.5.1 Objectives of the Error Analysis

The Air Force Geophysics Laboratory (AFGL) was tasked by the Space and Missiles Systems Organization (SAMSO) to forecast, sample, and report the ice, snow, and water particle environment for erosion testing of payloads launched from the NASA Wallops Flight Center. The mass concentrations of hydrometeors along the payload trajectory were estimated using radar data obtained from the NASA Space Range Radar (SPANDAR) at Wallops Island, VA. The radar reflectivity-to-mass concentration conversion relationships required to interpret the radar data were obtained from aircraft measurements made in the vicinity of the payload trajectory prior to launch.

The objective of the uncertainty (or error) analysis reported herein is to review the radar and aircraft measurement procedures and provide estimates of both the possible (maximum) and probable (most likely) error bounds (uncertainties) for the mass concentration estimates. This report does not provide error bound estimates for a particular launch but considers the kinds of uncertainties that could occur and provides estimates of their expected values. This analysis only considers uncertainties

that can occur when the equipment is operated correctly and does not mal-
function. In some cases, it is possible to detect operator or equipment
error but often it is not. Possible areas for improvement are pointed
out in the report but conscientiousness was expected of those involved in
the measurement program and is not questioned further.

2.5.2 Brief Description of the Measurement Program

Mass concentrations of ice, snow, and water particles encountered by
the test vehicle as it passed along its trajectory are required to evaluate
the susceptibility of nose tip and side wall materials to erosion. In
situ observations of mass concentration are not possible during vehicle
traversal. Remote observations by radar were obtained immediately prior
to, during, and after vehicle passage to best describe the hydrometeor
environment. These observations were converted to mass concentration
estimates using reflectivity-to-mass relationships derived from aircraft
samples of the hydrometeors prior to launch.

Measurements with SPANDAR were made to support the Sandia Air Force
Materials Study (SAMS) program during the 1975-1976 time period (SAI, 1976)
and to support the Materials Screening Vehicle (MSV) program during the
1976-1977 time period (Cockayne and Fletcher, 1976). For this report,
the differences between the two measurement programs are best described
by noting that the SAMS observations were made close to the radar (5-25
km range) while the MSV observations are made at significantly longer
ranges ($\sim$150 km).

Four separate types of radar observations were required for the ero-
sion measurement program: elevation scans over disdrometers and rain
gauges to provide primary radar calibration during a mission, sphere
tracks to provide secondary radar calibration, link-mode observations
with aircraft flights made just before launch to provide reflectivity-to-
mass conversion relationships, and volume scan observations along the
expected vehicle trajectory immediately preceding, during, and after
vehicle traversal through the erosion test region. These measurements
were supported by three digital processor systems attached to the radar
each of which must be separately calibrated. The radar operator (the
John Hopkins Applied Physics Laboratory-APL) maintained and operated a
minicomputer processing system that controlled the antenna and was used

6

to record the link-mode observations. AFGL maintained and operated the two other processors, one to provide primary data recording for post test analysis and the second to provide on site, near-real-time liquid water content estimates for mission control. The second processor also provided backup data recording for post test analysis.

The aircraft measurement program entailed the use of two aircraft operated by AFGL to obtain hydrometeor size, phase, and type distributions. Size distributions were obtained using PMS 1-dimensional (1-D) cloud and precipitation particle probes (Knollenberg, 1970). Crystal habit or particle phase and type information were obtained using PMS 2-D cloud and precipitation particle probes. The aircraft also recorded temperature, humidity, air speed and time data to aid in post test analysis.

Link-mode observations encompassed the simultaneous use of one of the aircraft and the radar to provide particle distribution and reflectivity measurements. SPANDAR automatically tracked the aircraft using its conical scan tracking system and sampled the reflectivity values one range interval closer to the radar than the interval occupied by the aircraft. In post analysis the aircraft and radar data were statistically compared. Although the data were taken simultaneously, the data sets were obtained from significantly different sampling volumes. The sampling volume for the aircraft probe is determined by the instrument capture area times the distance traversed by the aircraft as it obtained a sample. The radar sampling volume is determined by the antenna beam cross section generated as it rotated about the aircraft position while scanning to track the aircraft times the distance along the beam defined by the pulse length of the radar and subsequent radar integration.

The final link in the chain of observations and analyses required to produce mass concentration estimates from SPANDAR data was the analysis of the PMS 1-D probe observations to provide equivalent melted sphere size distributions from the observed particle shadow lengths. Given the equivalent melted sphere sizes and postulates about particle shape and orientation, the mass and reflectivity values may be calculated for use in generating the reflectivity-to-mass conversion relationships. The PMS probe does not directly sample the equivalent melted sphere diameter; it only records an estimate of the maximum size (length) of the projection of each particle onto a horizontal line perpendicular to the direc-

tion of aircraft motion as the particle passes through the sampling head. The probe does not provide any information on the other physical dimensions rquired for the calculation of a volume estimate or on the particle density required for the calculation of a mass estimate. Except for the PMS 2-D probe, the 1-D probe provides more relevant information about hydrometeors than any other instrument currently available.

The length-to-melted diameter (mass) conversion relationships for the PMS probes have been statistically determined using a two step process. First, the response of the particle measurement system to idealized particle shapes was simulated to provide corrections for habit, orientation, and size (Knollenberg, 1975). Second, a large number of observations of naturally occurring crystals were analyzed to determine the expected relationship between the maximum (horizontal) crystal dimension and particle mass. Separate relationships were developed for each crystal habit. To reduce the sensitivity of the reflectivity-to-mass conversion relationships to possible uncertainties associated with the identification of crystal habit and with the use of a limited number of observations to generate the required length-to-mass relationships, the PMS data were used only to calculate a multiplier to be used with the square root of the radar reflectivity values for the estimation of mass concentration (the "κ" factor) and not to provide direct estimates of either mass or reflectivity ("κ" is equal to the ratio of mass to the square root of reflectivity). The resultant reduction in sensitivity to sizing error however, depends upon the breadth of the particle size distribution.

Reduced to bare essentials, the radar was used to provide an estimate of the radar reflectivity factor, Z, and the aircraft measurements were used to provide the relationship between Z and the mass concentration as expressed by an equivalent liquid water content, M. The liquid water content was determined by

$$M = \kappa \sqrt{Z} \qquad (1\text{-}1)$$

Uncertainties in the estimation of liquid water content arise from two basic causes: equipment calibration and data interpretation. The total uncertainty for an M estimate is caused by both aircraft system and radar system uncertainties. In general, the largest contribution to the

8

total uncertainty budget is caused by data interpretation. In the extreme, the M value for pristine ice plates may differ by more than an order of magnitude from the M value for needles with the same Z value. For the widespread storms encountered during the measurement period, the occurrence of large regions with pristine crystals was rare and uncertainties of this magnitude are not anticipated.

2.5.3 Total Uncertainty Budget

The possible uncertainty sources and their contribution to the total liquid water content estimation uncertainty budget are listed in Table 1. The uncertainties are separated into radar and aircraft categories and further segregated into calibration and interpretation classes. The uncertainties for each category are listed by contribution to M using $M = \kappa\sqrt{Z}$. These categories are then subdivided into identifiable subclasses which are described in detail in this report. Uncertainty estimates are provided for SAMS and MSV missions. The difference between the two are due to differences in distance between the radar and the path of the vehicle through the erosion test region. In addition, uncertainty estimates are provided for observations at 4 heights. The crystal habits were assumed to be bullet rosettes at a 10 km height, small snow at 6 km, and large snow at 3 km height and wet snow at 2 km height (just above the melting layer).

The measurement uncertainties are assumed to be multiplicative and are given both in decibels and in percent (increase) of the estimated value. Three types of uncertainties are treated, bias (not subject to change over the entire observation period), slowly varying (not expected to change during a mission), and random (expected to change from one sample to the next). Slowly varying uncertainties are caused by such problems as not precisely setting or monitoring power levels in the radar set, not estimating the correct calibration constant, or not estimating the correct particle habit and size distribution for a given height region. Bias errors are of two possible sources: uncertainties in the values of absolute constants such as antenna gain that may exist even after a number of measurements to determine their values, and the use of incorrect values for constants in the calibration or data analysis procedures. Bias errors caused by the use of incorrect constants or procedures may be

TABLE 1b

MSV Missions (150 km Range): Contributions to Liquid Water Content Uncertainties

CATEGORY	2 km Height - Large Snow E. Bias+ dB	%	Slowly Vary dB	%	Random dB	%	3 km Height - Large Snow E. Bias+ dB	%	Slowly Vary dB	%	Random dB	%	6 km Height - Small Snow E. Bias+ dB	%	Slowly Vary dB	%	Random dB	%	10 km Height - Ice Crystals E. Bias+ dB	%	Slowly Vary dB	%	Random dB	%
RADAR - $\sqrt{Z}$																								
Calibration	0.2	5	0.5+	12	0.2	5	0.2	5	0.5+	12	0.2	5	0.2	5	0.5+	12	0.2	5	0.2	5	0.5+	12	0.2	5
Interpretation																								
Attenuation	-	-	0.3+	7	-	-	-	-	0.2+	5	-	-	-	-	0.1+	2	-	-	-	-	0.1+	2	-	-
Polarization	-	-	-	-	-	-	-	-	-	-	-	-	-	-	0.5	12	-	-	-	-	0.5	12	-	-
Side Lobes	-	-	5.0	216	-	-	-	-	2.0	58	-	-	-	-	0.1	2	-	-	-	-	0.1	2	-	-
Refraction	-	-	1.4	38	-	-	-	-	0.8	20	-	-	-	-	0.6	15	-	-	-	-	0.5	12	-	-
Range Errors	-	-	-	-	-	-	-	-	-	-	-	-	-	-	-	-	-	-	-	-	-	-	-	-
AIRCRAFT - κ																								
Calibration	-	-	0.1	2	-	-	-	-	0.1	2	-	-	-	-	0.1	2	-	-	-	-	0.1	2	-	-
Interpretation																								
Length-to-Mass	-	-	0.2	5	-°	-	-	-	0.2	5	-°	-	-	-	0.3	7	-°	-	-	-	0.8	20	-°	-
Crystal Habit	-	-	1.2	32	-°	-	-	-	1.2	32	-°	-	-	-	1.4	38	-°	-	-	-	3.6	140	-°	-
Truncation	-	-	2.2	66	-	-	-	-	0.1	2	-	-	-	-	0.1	2	-	-	-	-	0.1	2	-	-
Sampling	-	-	2.9	95	-°	-	-	-	0.3	7	-°	-	-	-	0.2	5	-°	-	-	-	0.1	2	-°	-
κ/Z	-	-	1.0	26	-°	-	-	-	1.0	26	-°	-	-	-	1.0	26	-°	-	-	-	1.0	26	-°	-
TOTAL - M = $\kappa\sqrt{Z}$	0.2	5	6.6	357	-°	-	0.2	5	2.7	86	-°	-	0.2	5	2.0	58	-°	-	0.2	5	3.9	145	-°	-

+ Correlated from one height to the next

° Random errors have been removed by averaging

TABLE 1a

SAMS Missions (25 km Range):
Contributions to Liquid Water Content Uncertainties

CATEGORY	2 km Height - Large Snow						3 km Height - Large Snow						6 km Height - Small Snow						10 km Height - Ice Crystals					
	E. Bias+		Slowly Vary		Random		E. Bias+		Slowly Vary		Random		E. Bias+		Slowly Vary		Random		E. Bias+		Slowly Vary		Random	
	dB	%	dB	%	dB	%	dB	%	dB	%	dB	%	dB	%	dB	%	dB	%	dB	%	dB	%	dB	%
RADAR - √Z																								
Calibration	0.2	5	0.5+	12	0.2	5	0.2	5	0.5+	12	0.2	5	0.2	5	0.5+	12	0.2	5	0.2	5	0.5+	12	0.2	5
Interpretation																								
Attenuation	0.3*	7	0.05+	1	-	-	0.3*	7	0.04	1	-	-	0.2*	5	0.02	-	-	-	0.2*	5	0.02	-	-	-
Polarization	-	-	-	-	-	-	-	-	-	-	-	-	-	-	0.5	12	-	-	-	-	0.5	12	-	-
Side Lobes	-	-	-	-	-	-	-	-	-	-	-	-	-	-	-	-	-	-	-	-	-	-	-	-
Refraction	-	-	-	-	-	-	-	-	-	-	-	-	-	-	-	-	-	-	-	-	-	-	-	-
Range Errors	0.3*+	7	0.1*+	2	-	-	0.4*+	10	0.1*+	2	-	-	0.7*+	17	0.2*+	5	-	-	0.6*+	15	0.2*+	5	-	-
AIRCRAFT - κ																								
Calibration	-	-	0.1	2	-	-	-	-	0.1	2	-	-	-	-	0.1	2	-	-	-	-	0.1	2	-	-
Interpretation																								
Length-to-Mass	-	-	0.2	5	-°	-	-	-	0.2	5	-°	-	-	-	0.3	7	-°	-	-	-	0.8	20	-°	-
Crystal Habit	-	-	1.2	32	-°	-	-	-	1.2	32	-°	-	-	-	1.4	38	-°	-	-	-	3.6	140	-°	-
Trucation	-	-	2.2	66	-°	-	-	-	0.1	2	-°	-	-	-	0.1	2	-	-	-	-	0.1	2	-°	-
Sampling	-	-	2.9	95	-°	-	-	-	0.3	7	-°	-	-	-	0.2	5	-°	-	-	-	0.1	2	-°	-
κ/Z Extrapolation	-	-	1.0	26	-°	-	-	-	1.0	26	-°	-	-	-	1.0	26	-°	-	-	-	1.0	26	-°	-
TOTAL - M = κ√Z	0.8	20	4.0	151	-°	-	0.9	23	1.7	48	-°	-	1.1	29	1.9	55	-°	-	1.0	26	3.9	145	-°	-

*Uncertainty may be removed by reprocessing the data

+Correlated from one height to the next

°Random errors have been removed by averaging

eliminated but bias errors caused by uncertainties in aboslute constants cannot be. Uncertainties that can be eliminated by reprocessing the available data are identified by asterisks (*) in the dB columns of Table 1.

Slowly varying uncertainties are statistical in nature and are assumed to have a log-normal distribution (log-normal since the uncertainties are multiplicative). The uncertainties for any category are considered to have a log-normal distribution which is described by the standard deviation of the logarithm (decibel value). The composite uncertainty is the sum of a number of independent uncertainties, hence, is calculated using the sum of the variances for each category (expressed in decibels).

The bias uncertainties are not random and must be treated in a different manner. Following Crane (1971), the maximum possible uncertainty for each category is summed to provide an estimate of the total maximum possible uncertainty. Again the logarithm of the uncertainty is used (decibel value) since the uncertainties are multiplicative. The maximum possible uncertainty is interpreted as being the equivalent of the 3-σ or three standard deviation value. To express the bias uncertainty as an expected uncertainty, one third the maximum possible value is used for entry in Table 1. The one third value is labeled E Bias for expected bias value to indicate that it does not correspond to the full maximum possible bias error value. The total error bounds for the measurements are obtained by combining the expected uncertainties using the sums of the squares of the statistically estimated components. The resultant error bounds are summarized in Table 2.

2.5.4 Uncertainties in the Estimate of the Environmental Severity Index

The analysis of uncertainties presented in this report primarily address the problem of estimating mass concentration values. Rain erosion analysts use the mass concentration estimates to model integrated effects. Their interest is not in the error at a point but in the error of integrals such as the Environmental Severity Index (ESI). ESI is defined as

$$ESI = \int_0^\infty M(h)h\,dh \qquad (1-2)$$

12

TABLE 2

MOST PROBABLE UNCERTAINTY BOUNDS FOR LIQUID WATER CONTENT ESTIMATES

Mission	Height (km)	68 Percent Errors Bounds		
		dB	factor	percent
SAMS	3.0	±1.9	$(1.55)^{\pm 1}$	-35,+55
	6.0	±2.2	$(1.66)^{\pm 1}$	-40,+66
	10.0	±2.5	$(1.78)^{\pm 1}$	-44,+78
MSV	3.0	±2.7	$(1.86)^{\pm 1}$	-46,+86
	6.0	±2.0	$(1.58)^{\pm 1}$	-37,+58
	10.0	±2.3	$(1.70)^{\pm 1}$	-41,+70

where M(h) is the particle mass concentration at height h (along the trajectory). The uncertainty (error) in ESI, ΔE, is linearly related to the error in mass concentration ΔM by

$$ESI + \Delta E = \int_0^\infty (M(h) + \Delta M(h))hdh$$

(1-3)

or $\qquad \Delta E = \int_0^\infty \Delta M(h)hdh$

The errors in mass concentration are multiplicative and best expressed by the ratio $\Xi_m = \Delta M/M$ (in decibels or percent). Therefore,

$$\Delta E = \int_0^\infty (\frac{\Delta M}{M})Mhdh = \int_0^\infty \Xi_m Mhdh$$

(1-4)

The bias component of the error is constant over space (h) and does not vary in time or from mission to mission. The bias error in ESI, ΔE_B, therefore, is given by

$$\Delta E_B = (\Xi_m)_B \int_0^\infty Mhdh = (\Xi_m)_B \cdot ESI$$

(1-5)

or $\qquad (\Xi_E)_B = (\Xi_m)_B$

The ESI or any other linear integral function of M therefore has a bias error equal in percent (or decibels) to the bias error in M.

The random error is due primarily to sampling errors associated with the radar measurements. This component of error is assumed to be uncorrelated from sample to sample and can be reduced by averaging. The integral for ESI can be reduced to a summation over samples

$$ESI = \int_0^\infty Mhdh \approx \sum_{j=1}^{J} (\sum_{i=1}^{I_j} \frac{M_{ij}}{I_j}) h_j \Delta h = \sum_{j=1}^{J} \overline{M}_j h_j \Delta h$$

(1-6)

where I_j samples are averaged for the jth layer and J layers are summed to provide an ESI estimate. The error is again given by

$$\Delta E = \sum_{j=1}^{J} [\sum_{i=1}^{Ij} \frac{(\Xi_m)_{ij}}{I_j}] \, \overline{M}_j h_j \Delta h$$

Since the errors are assumed to be statistically independent from sample to sample, the expected square error is given by

$$(\Delta E_R)^2 = \sum_{j=1}^{J} \sum_{i=1}^{I_j} (\frac{(\Xi_m)_{Rj}}{I_j})^2 (\overline{M}_i h_j \Delta h)^2 = \sum_{j=1}^{J} \frac{[(\Xi_m)_{Rj}]^2}{I_j} (\overline{M}_j h_m \Delta h)^2$$

and the rms error, ΔE_R is given by

$$\Delta E_R = \sqrt{ \sum_{j=1}^{J} \frac{[(\Xi_m)_{Rj}]^2}{I_j} \overline{M}_j{}^2 h_j{}^2 } \; \Delta h \qquad\qquad (1-7)$$

If $\overline{M}_j$ varies inversely with height, $\overline{M}_j h_j$ = constant = $M_o h_o$ and if $(\Xi_m)_R$ and $I_j = I$ are not dependent on h, the rms error would be given by

$$\Delta E_R = \frac{(\Xi_m)_R M_o h_o \, h}{\sqrt{JI}} \qquad\qquad (1-8)$$

where JI is the number of samples. In general, $\overline{M}_j$ does not vary inversely with height and the reduction in sampling error is not as great as expressed by (1-8).

Intermediate between the random errors and bias errors are the slowly varying errors. These errors are correlated at each height level but may be uncorrelated from one height to the next. Errors which are caused by uncertainties in setting radar parameters are correlated from one height to another but vary from one mission to another. Errors associated with the incorrect choice of crystal habit are correlated over the depth of a layer with a particular habit but uncorrelated between layers with different habits. The slowly varying error, therefore, is given by

$$\Delta E_s = \sqrt{ \sum_{j=1}^{J} [(\Xi_m)_{sj}]^2 \overline{M}_j{}^2 h_j{}^2 \Delta h^2 + \sum_{j=1}^{J} \sum_{\substack{k=1 \\ k \neq j}}^{J} (\Xi_m)_{sj} (\Xi_m)_{sk} \rho_{jk} \overline{M}_j \overline{M}_k h_j h_k \Delta h^2 }$$

$$(1-9)$$

15

where ρ_{jk} is the correlation coefficient between observations at levels j, and k. This can be approximately reduced to the sum over independent layers, typically 2 to 4, representative of each habit where the correlation coefficient ρ_{ik} is 1 within the layer and zero from layer to layer:

$$\Delta E_s \simeq \sqrt{\sum_{j=1}^{J^*} (\Xi_m)_{sj}^2 \, \overline{M}_j^2 \, h_j^2 \, \Delta h^2} \qquad (1\text{-}10)$$

where J* is the number of independent layers (layers with different habit).

Referring to Table 1, the bias errors and the slowly varying errors which are correlated from height to height are also errors in ESI. The random errors may be reduced by summing over many samples, hence, do not contribute to the error in estimating ESI. The slowly varying errors which are uncorrelated from layer-to-layer (habit-to-habit) can be reduced only if the mass concentration is inversely related to height otherwise, the effect of the weighting by $\overline{M}_i h_j$ must be taken into account when computing the error. Using the sample M(h) distribution given in Figure 1, the errors for ESI computed using the error estimates given in Table 1 are given in Table 3.

TABLE 3

ESI ESTIMATES*

	Bias (dB)	Slowly Varying (dB)	Total (dB)	Total Percent
SAMS	1.0	1.8	±2.1	-38, +62
MSV	0.2	2.4	±2.4	-42, +74

*ESI value calculated for measurements at heights above 3 km.

16
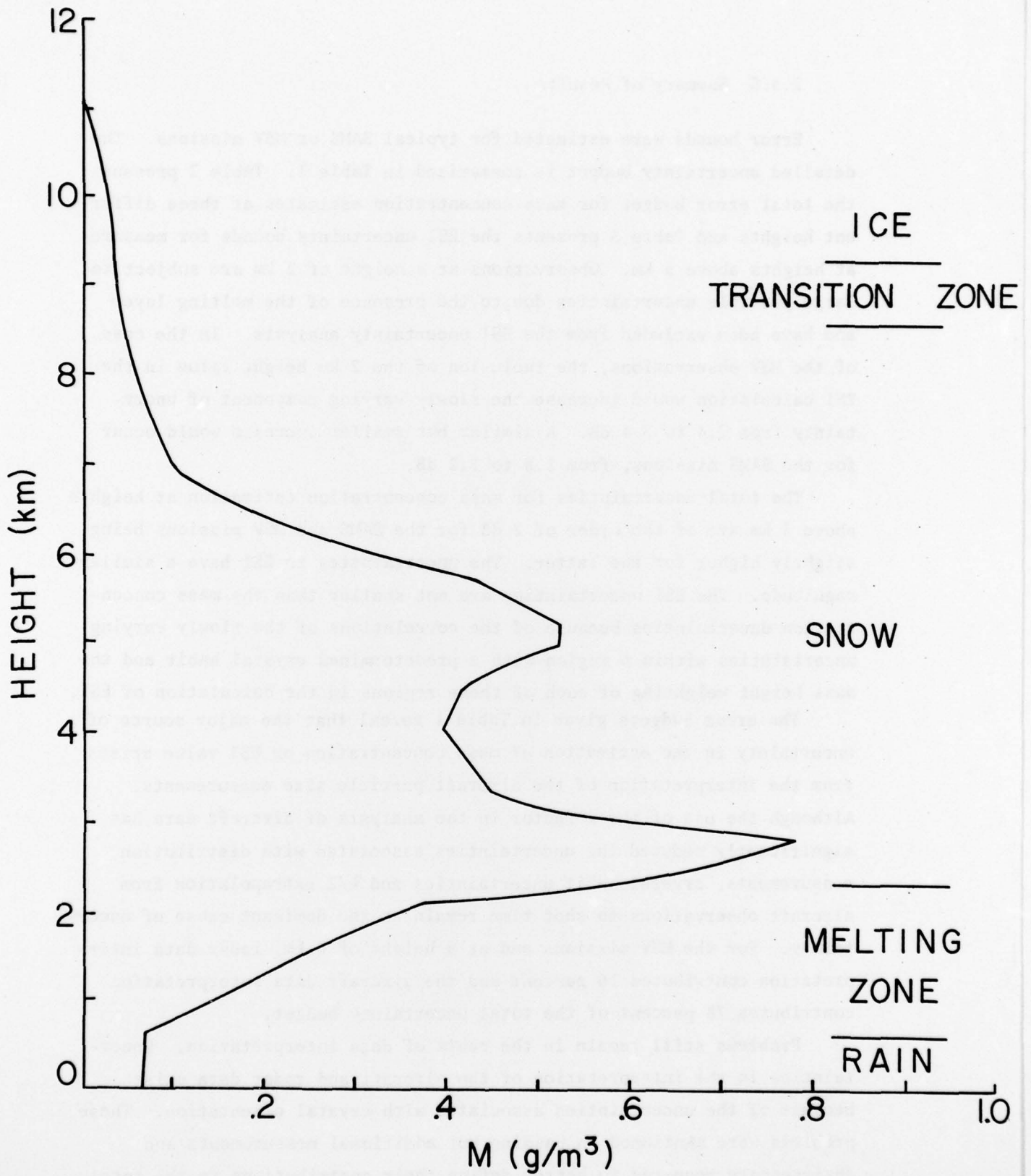
Figure 1   Mass Concentration Profile, M(h), for MSV-2 Test, 20 March 1976

2.5.5 Summary of Results

Error bounds were estimated for typical SAMS or MSV missions. The detailed uncertainty budget is summarized in Table 1. Table 2 presents the total error budget for mass concentration estimates at three different heights and Table 3 presents the ESI uncertainty bounds for measure- at heights above 3 km. Observations at a height of 2 km are subject to large possible uncertainties due to the presence of the melting layer and have been excluded from the ESI uncertainty analysis. In the case of the MSV observations, the inclusion of the 2 km height value in the ESI calculation would increase the slowly varying component of uncer- tainty from 2.4 to 3.4 dB. A similar but smaller increase would occur for the SAMS missions, from 1.8 to 2.2 dB.

The total uncertainties for mass concentration estimation at heights above 3 km are of the order of 2 dB for the SAMS and MSV missions being slightly higher for the latter. The uncertainties in ESI have a similar magnitude. The ESI uncertainties are not smaller than the mass concen- tration uncertainties because of the correlations of the slowly varying uncertainties within a region with a predetermined crystal habit and the mass height weighting of each of these regions in the calculation of ESI.

The error budgets given in Table 1 reveal that the major source of uncertainty in the estimation of mass concentration or ESI value arises from the interpretation of the aircraft particle size measurements. Although the use of the κ factor in the analysis of aircraft data has significantly reduced the uncertainties associated with distribution measurements, crystal habit uncertainties and κ/Z extrapolation from aircraft observations to shot time remain as the dominant cause of uncer- tainty. For the MSV missions and at a height of 6 km, radar data inter- pretation contributes 16 percent and the aircraft data interpretation contributes 78 percent of the total uncertainty budget.

Problems still remain in the realm of data interpretation. Uncer- tainties in the interpretation of the aircraft and radar data exist because of the uncertainties associated with crystal orientation. These problems were mentioned in passing but additional measurements and analyses are required to better define their contributions to the total error budget. The reported tendency for the wide arm precipitation probe

18

to still undersize particles after the inclusion of recommended corrections also requires additional experimental verification and analysis.

2.6 Task 6 - A Study of Thin Cirrus Over the Tropical Pacific

As part of the overall project, Burke, et al (1978) have carried out a theoretical study of the detectability of high altitude (>10 km) thin cirrus clouds by various remote sensors over the tropical Pacific. Defining the existence and probability of occurrence of thin c·rus clouds is important because of the requirement that there be a natural transition from laminar to turbulent flow over reentering objects, which normally occurs around 10 km. Microscopic roughening of the RV surface caused by impact of isolated hydrometeors can be sufficient to trigger transition and thereby to invalidate the experiment. According to one estimate, there will be an intolerable risk of premature transition above a 10 km height whenever particles larger than 80 microns occur in concentrations of more than 1 m^{-3}. A "severe-clear" case or the absence of any detectable ice particles is therefore required above 10 km.

Because of the sparsity of direct measurements, it is difficult to define the atmospheric environment in the vicinity of reentering vehicles for the purpose of evaluating natural atmospheric effects on them. The attempt of identifying cirrus clouds along reentry paths is further complicated by the multiple of their possible crystal sizes, shapes, orientations, numbers and densities. Consequently, a sensitivity study of various remote sensing techniques for quantitative measurements of thin cirrus clouds is required.

The advantage of using remote sensors is that they provide continuous information on cirrus properties in the vicinity of actual reentries. Using in situ measurements in the reentry area, on the other hand, can cause possible dangers from the reentering object. However, remote sensors provide only certain quantities that are often difficult to relate uniquely to standard atmospheric parameters. Assumptions have to be made in order to retrieve all the cirrus cloud quantities: height, thickness, ice water content, crystal size and concentrations, etc. Theoretical estimates, based on optical properties of ice crystals and radiative transfer computations, are carried out to predict the minimum detectable number density of ice crystals for various remote sensors.

The standard tropical atmosphere is used as ambient conditions to simulate Kwajalein atmosphere. The various remote sensors discussed in the Burke, et al. report include (1) eyeball detection at surface, (2) eyeball detection from aircraft altitude, and (3) infrared (6.7 μm wavelength) sensor from space.

The conclusions of the study were as follows:

- from theoretical computations it has been shown that thin cirrus cloud detected from aircraft observations or infrared sensors on-board satellites can be invisible from the ground;

- the required concentration of less than 1 m^{-3} of ice particles greater than 80 μm is too low a threshold (by a factor of 10^3) for virtually all the existing sensors; and

- a probability study provided a statistical review of the severe clear cases; such severe clear cases are not established from the threshold of 1 m^{-3} of particles greater than 80 μm but from observations of cirrus combined with various meteorological criteria.

3. REFERENCES

Burke, H.K., K.R. Hardy and A.J. Bussey (1978): "Thin Cirrus Cloud Over the Tropical Pacific", Scientific Report No. 3, AFGL-TR-78-0259, ERT, Concord, Mass.

Bussey, A.J. (1978): "A Methodology for Cross Section Analysis and Liquid Water Content Assessment at Kwajalein", Scientific Report No. 2, AFGL-TR-78-XXXX, ERT, Concord, Mass.

Cockayne, J.E. and A.A. Fletcher (1976): "Hydrometeor Measurement Operations Plan for AFGL Support of SAMSO MSV Erosion Tests at NASA Wallops Flight Center in 1976-1977", Science Applications, Inc., McLean, Virginia.

Crane, R.K. (1971): "Description of the Avon-to-Westford Experiment", Tech. Rept. 483, MIT Lincoln Laboratory, Lexington, Mass.

Crane, R.K. (1978): "Evaluation of Uncertainties in the Estimation of Hydrometeor Mass Concentrations Using SPANDAR Data and Aircraft Measurements", Scientific Report No. 1, AFGL-TR-78-0118. ERT, Concord, Mass.

Knollenberg, R.G. (1970): "The Optical Array: An Alternative to Extinction and Scattering for Particle Size Measurements", J. Appl. Meteor., 9, 86-103.

Knollenberg, R.G. (1975): "The Response of Optical Array Spectrometers to Ice and Snow: A Study of Probe Size to Crystal Mass Relationships", Sci. Rept. No. 1, AFCRL-TR-75-0444, Particle Measuring Systems, Inc., Boulder, Colorado.

SAI (1976): "Operations Plan for AFCRL Support of ABRES Erosion Tests at NASA Wallops Flight Center, Winter of 1975-1976", Science Applications, Inc., McLean, Virginia.